Chirp-Based Impedance Spectroscopy

A Wideband Alternative to Traditional Sinusoidal Methods

Adam Gottesman
Methodology Development, Embedded Firmware and Circuit Design

Georgi Korchakov
PCB Layout, Circuit Design and Simulation Analysis

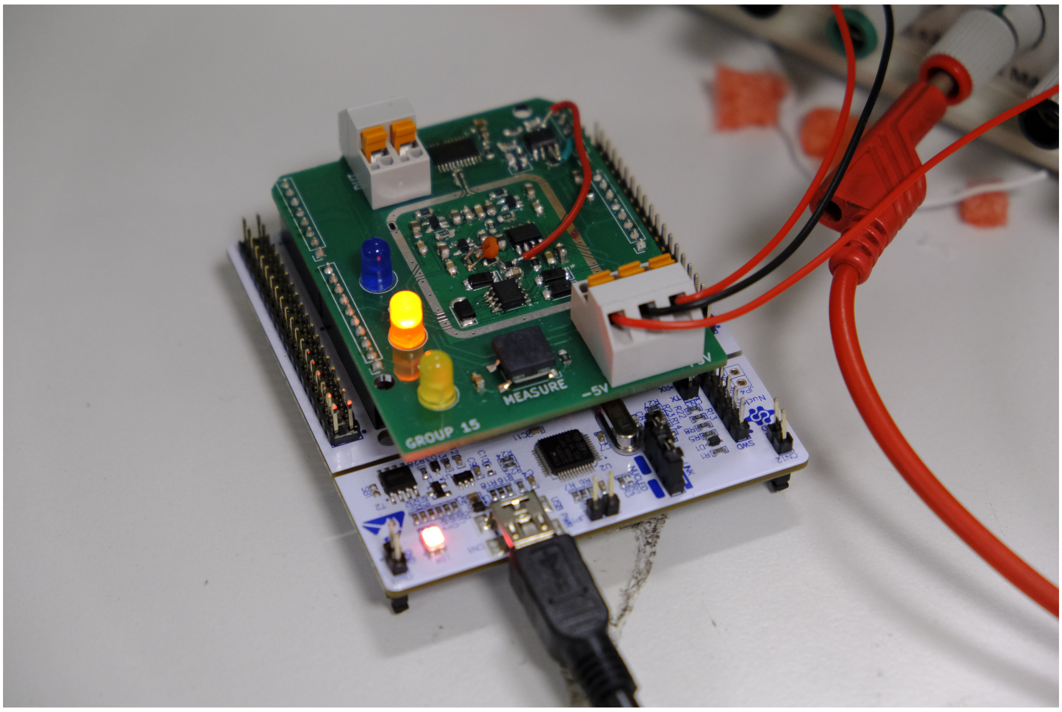

Imperial College London

March 2025

Contents

1 Methodology of Impedance Spectroscopy

The impedance measurement system follows the I-V method, employing the Nucleo to generate an excitation signal, acquire voltage and current waveforms, and compute the impedance in real-time. The excitation signal is outputted via the 12-bit DAC of the Nucleo STM32F446RE and applied to the Device Under Test (DUT) through a filtering stage to suppress high-frequency noise. The corresponding voltage and current responses are sampled synchronously at 250 kHz using three ADC channels, ensuring that the full excitation bandwidth is captured without exceeding the available memory constraints.

The current flowing through the DUT is indirectly obtained using a known reference resistor R_{range}, placed in series with the DUT. The system measures three voltages:

- the excitation voltage before the reference resistor, $V_{\text{in}}(t)$,
- the raw voltage drop across the reference resistor, $V_{\text{raw}}(t)$, and
- the offset voltage from the feedback configuration of the custom instrumentation amplifier, $V_{\text{offset}}(t)$.

The offset-corrected voltage across the reference resistor is then calculated as:

$$V_{\text{range}}(t) = V_{\text{raw}}(t) - V_{\text{offset}}(t), \tag{1}$$

and the current through the DUT is computed as:

$$I(t) = \frac{V_{\text{range}}(t)}{R_{\text{range}}}. \tag{2}$$

The voltage across the DUT is determined as:

$$V_{\text{DUT}}(t) = V_{\text{in}}(t) - V_{\text{range}}(t). \tag{3}$$

Once the voltage and current waveforms are acquired, they are transformed into the frequency domain using the Discrete Fourier Transform (DFT). This operation provides the complex spectra $V(f)$ and $I(f)$, from which the frequency-dependent impedance is computed as:

$$Z(f) = \frac{V(f)}{I(f)}. \tag{4}$$

Since a wideband signal excites the DUT with all relevant frequencies in a single acquisition, the impedance magnitude can be directly extracted as:

$$|Z(f)| = \left| \frac{V(f)}{I(f)} \right|. \tag{5}$$

Additionally, the phase response of the impedance is computed as:

$$\theta(f) = \arg\left(\frac{V(f)}{I(f)} \right). \tag{6}$$

2 Chirp-Based Excitation

Chirp-based excitation enables wideband measurement in a single acquisition, eliminating the need for sequential frequency sweeps. By applying an appropriate chirp signal and performing a Fourier Transform on the measured response, the impedance can be computed simultaneously across a wide bandwidth.

2.1 Linear Chirp

The simplest chirp signal, presented in Figure 1, is the Linear Chirp, which increases in frequency uniformly over time. This ensures that all frequencies within the desired range are excited equally. Mathematically, the signal is given by:

$$s_{\text{linear}}(t) = A_0 \cos\left(2\pi \left(f_0 t + \frac{k}{2} t^2 \right) \right), \tag{7}$$

where:

- A_0 is the amplitude scaling factor.
- f_0 is the initial frequency at $t = 0$.
- $k = \frac{f_1 - f_0}{T}$ is the chirp rate, which controls how rapidly the frequency increases.
- T is the total chirp duration.

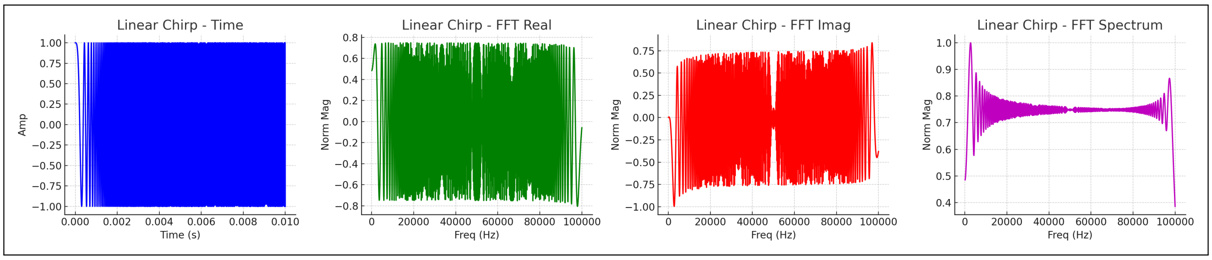

Figure 1: Time and frequency-domain characteristics of the Linear Chirp.

While the Linear Chirp features full-band excitation, its constant amplitude introduces sharp transitions at the waveform boundaries. This leads to spectral leakage, contaminating the frequency-domain response with undesired artefacts. To mitigate these effects, a Tapered Linear Chirp signal is also considered.

2.2 Tapered Linear Chirp

The Tapered Linear Chirp, shown in Figure 2, smoothly transitions between frequencies while minimising spectral artefacts. It follows a linear frequency sweep while its amplitude is modulated by a Gaussian envelope. Mathematically, the signal is given by:

$$s_{\mathrm{TLC}}(t) = A_0 e^{-\alpha\left(t-\frac{T}{2}\right)^2} \cos\left(2\pi\left(f_0 t + \frac{k}{2}t^2\right)\right), \tag{8}$$

where:

- A_0 is the amplitude scaling factor.
- α controls the Gaussian tapering, determining how quickly the amplitude decays.
- f_0 is the initial frequency.
- $k = \frac{f_1 - f_0}{T}$ is the chirp rate.
- T is the total chirp duration.

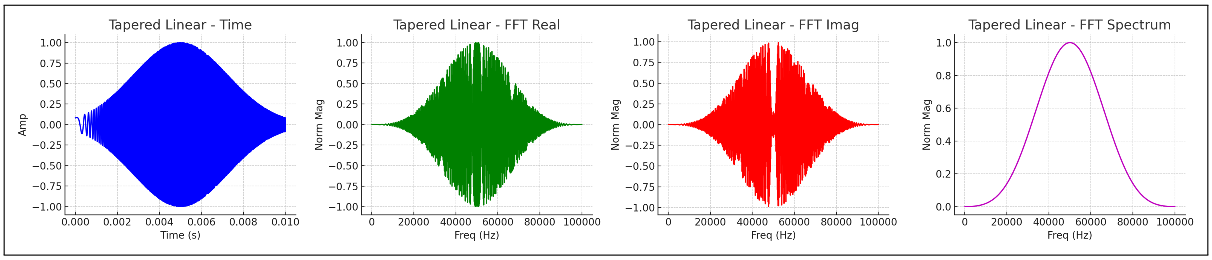

Figure 2: Time and frequency-domain characteristics of the Tapered Linear Chirp.

2.3 Limitations of the Tapered Linear Chirp

The Tapered Linear Chirp significantly improves measurement quality by reducing spectral leakage compared to standard linear chirps. However, practical implementation of a complex impedance measurement device using this method revealed notable limitations, particularly in accurately characterising reactive components such as inductors and capacitors. Investigation into these limitations identified the inherent quadratic-phase accumulation within the chirp signal as a fundamental obstacle.

2.4 Quadratic Phase Accumulation

Although the instantaneous frequency of the Tapered Linear Chirp increases linearly with time, the instantaneous phase accumulates quadratically [1]. Mathematically, the instantaneous frequency is expressed as:

$$f_{\text{inst}}(t) = f_0 + kt, \tag{9}$$

while the resulting instantaneous phase is described explicitly by separating the linear and quadratic components:

$$\phi(t) = 2\pi f_0 t + \pi k t^2. \tag{10}$$

Here, the first term represents linear phase accumulation, whereas the second term explicitly represents the quadratic-phase component.

This quadratic-phase accumulation disperses the chirp's energy across its duration, leading to a broad temporal distribution of spectral content. This dispersion complicates the accurate extraction of frequency-domain information through Fourier Transform-based impedance calculations. Specifically, resolving reactive components, characterised by frequency-dependent phase shifts, becomes particularly problematic. This limitation significantly affects measurement precision and reliability for reactive elements.

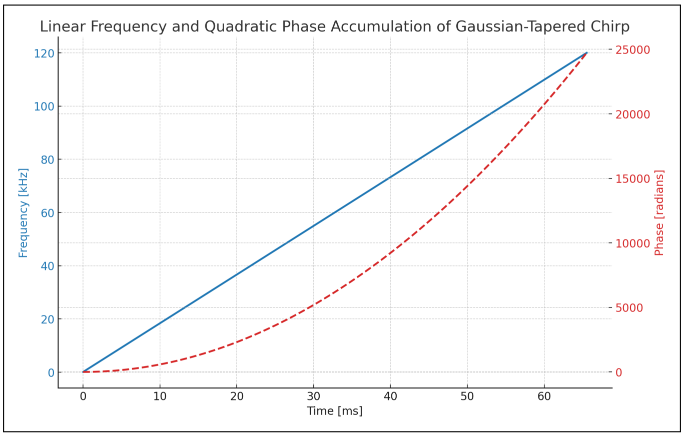

Figure 3: Linear frequency versus quadratic phase accumulation.

2.5 Phase Correction via Pulse Compression

To overcome the identified limitations, pulse compression is proposed as a promising future improvement [2]. Pulse compression utilises matched filtering to counteract quadratic-phase dispersion effectively, concentrating the chirp energy into a sharply defined, impulse-like response.

2.5.1 Matched Filtering Principle

Matched filtering involves correlating the measured signal $x(t)$ with a known reference chirp $h(t)$. Mathematically, this correlation is represented as convolution with the complex conjugate of the reference signal:

$$y(t) = x(t) * h^*(-t). \tag{11}$$

In the frequency domain, this convolution simplifies to multiplication:

$$Y(f) = X(f) \cdot H^*(f). \tag{12}$$

Applying the inverse Fourier transform yields the compressed time-domain signal:

$$y(t) = \mathcal{F}^{-1}\{Y(f)\}. \tag{13}$$

2.5.2 Expected Benefits

Employing pulse compression is expected to dramatically reduce temporal dispersion, providing a highly localised impulse-like response. This improvement should enable more precise resolution and clearer differentiation of impedance characteristics, significantly enhancing measurement accuracy for reactive components. Figure 4 illustrates the anticipated transformation from the original dispersed chirp into a focused virtual impulse, highlighting the potential effectiveness of this approach as a future enhancement.

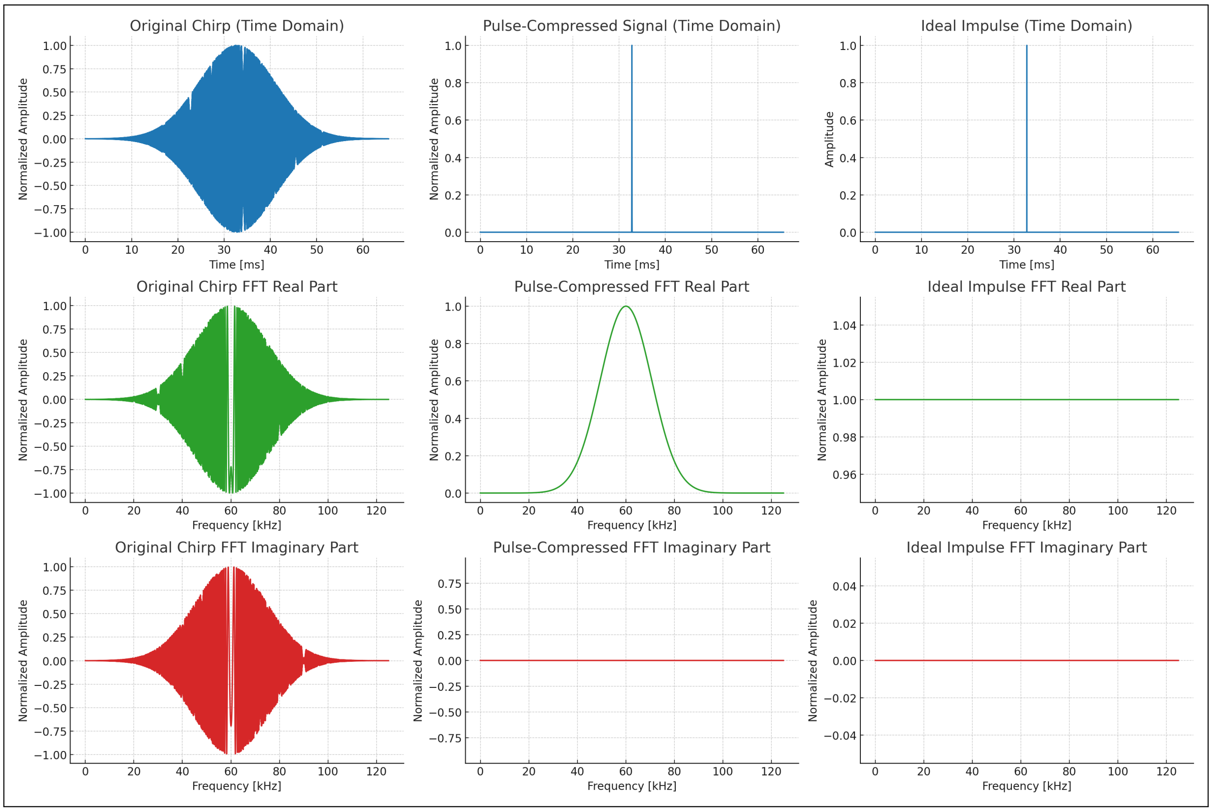

Figure 4: Time-frequency comparison: original chirp, pulse-compressed chirp, and ideal impulse.

3 Excitation Synthesis

Since the excitation signal is generated using the Nucleo STM32F446RE's 12-bit DAC, and the available RAM (∼130 kB) limits storage capacity, chirps are precomputed and stored in a 16,384-sample Look-Up Table (LUT), clocked at 1 MHz. The ADC captures the response at 250 kHz, yielding 4,096 samples per acquisition.

To assess the effectiveness of different excitation signals, MATLAB simulations were performed on both the Linear Chirp and the Tapered Linear Chirp (see Figure 5). The Linear Chirp produced a relatively uniform broadband response but exhibited spectral artefacts due to its abrupt onset and the discrete nature of the LUT. In contrast, the Tapered Linear Chirp, with its smooth amplitude envelope, significantly reduced spectral leakage.

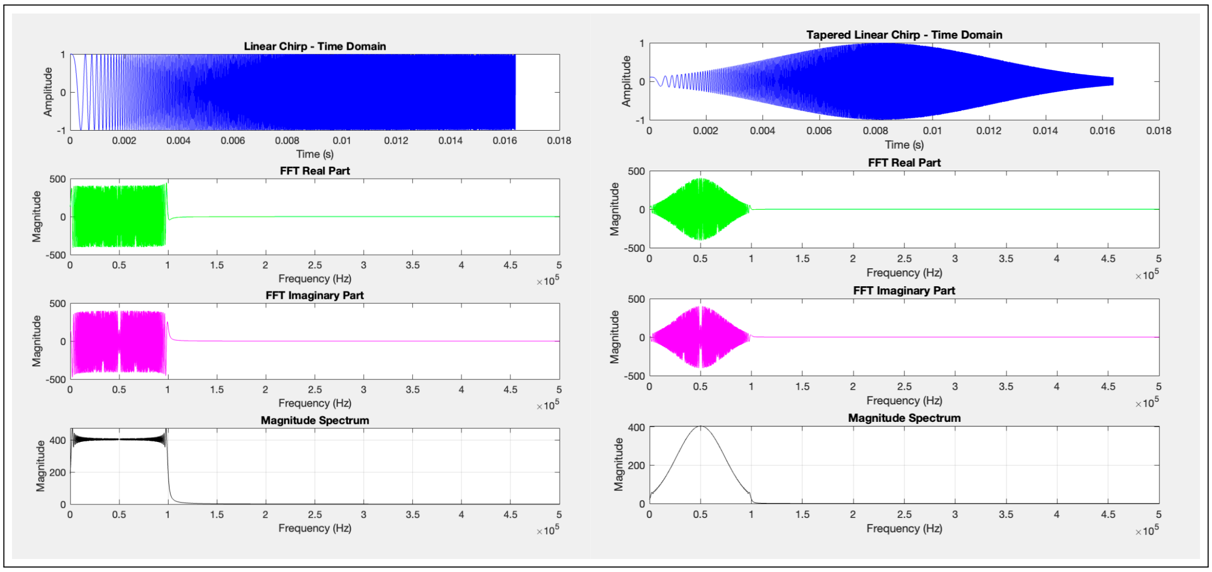

Figure 5: MATLAB simulations of synthesised chirps.

4 Updated Digital Implementation

The impedance measurement system operates in a structured sequence designed to ensure a precise and reliable characterisation of the Device Under Test (DUT). This implementation employs a bare-metal approach using the Cortex Microcontroller Software Interface Standard (CMSIS), providing direct, low-level access to hardware registers and peripherals. The CMSIS implementation ensures optimised performance, minimal overhead, and enhanced control, critical for high-speed data acquisition and precise timing synchronisation.

Initially, the system performs comprehensive hardware and peripheral initialisation, configuring the Digital-to-Analog Converter (DAC), Analog-to-Digital Converters (ADCs), Direct Memory Access (DMA) channels, timers, and Look-Up Table (LUT) containing the Gaussian-Tapered Linear Chirp excitation signal.

Following system initialisation, the device enters an idle state, awaiting user interaction. Upon pressing the measurement initiation button, an interrupt service routine (ISR) is triggered, activating two timers: one driving the DAC at a sampling rate of 1 MHz and another triggering the ADCs at 250 kHz. Simultaneously, DMA channels become active, facilitating the transfer of precomputed waveform data from the LUT buffer to the DAC output and transferring sampled ADC data to designated memory buffers.

The DAC outputs the Gaussian-Tapered Linear Chirp excitation signal, while the three synchronised ADC channels capture the voltage and current waveforms associated with the DUT. The LUT buffer comprises 16384 (4×4096) samples, aligning with the ADC buffers containing 4096 samples, ensuring simultaneous completion of both output and input operations.

Upon filling the ADC buffers, a DMA interrupt is activated, signaling the completion of data acquisition. The interrupt handler subsequently disables both DAC and ADC timers to halt signal generation and sampling processes. The acquired data undergoes evaluation to determine if autoranging criteria are met.

If the autoranging criteria are not satisfied, adjustments to the measurement range resistor and programmable gain amplifier (PGA) settings are applied as part of the autoranging process, and the measurement cycle repeats until suitable conditions are met.

Finally, the captured voltage and current data is processed to compute the DUT impedance using the established I-V methodology. Frequency-domain analysis is currently performed via Fast Fourier Transform (FFT) to calculate the complex impedance. Additionally, the matched filtering technique is planned to be implemented in future enhancements to eliminate dispersion by concentrating the chirp energy into a sharply defined, impulse-like response. The computed impedance results, including magnitude and phase, are subsequently displayed or outputted for further analysis.

After completing the measurement cycle and presenting the results, the system returns to the idle state, ready to initiate the next measurement upon user command.

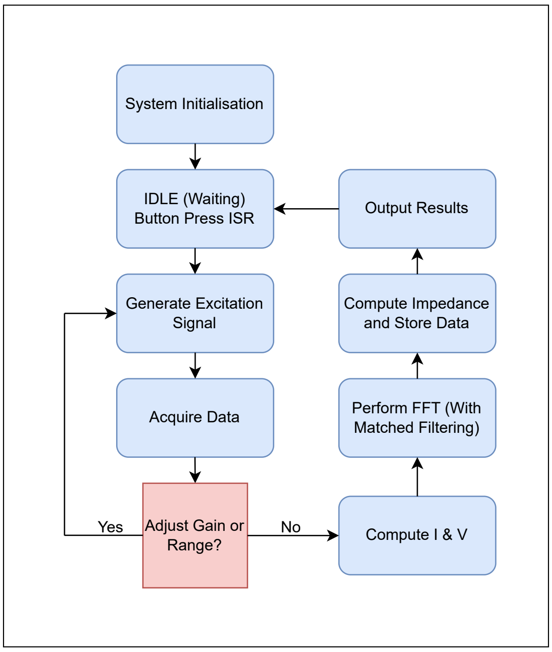

Figure 6: Digital implementation flowchart.

5 Final Schematic

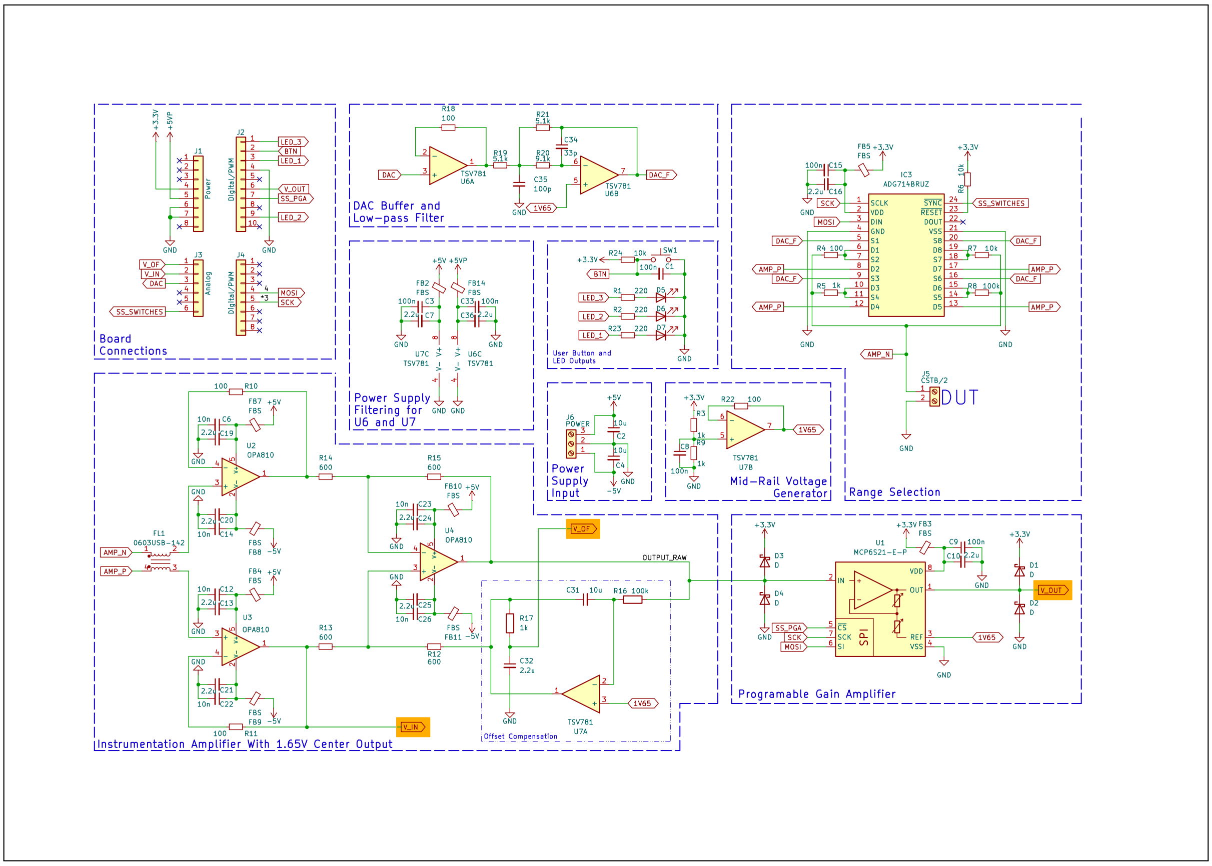

Figure 7: Final Schematic.

References

[1] Christos Papavassiliou, Personal Communication regarding Quadratic Phase Dispersion in Chirp Signals, Imperial College London, March 2025.

[2] Ayush Bhandari, Personal Communication on Pulse Compression, Imperial College London, March 2025.